Development of a CFD model for catalytic recombination of hydrogen and oxygen in a packed bed reactor

Sachin Kamath*, Sandeep K C, Kalyan Bhanja
Heavy Water Division, Chemical Engineering Group, BARC

ABSTRACT

Oxygen production has become a crucial process to meet the increasing demand of medical grade oxygen during the current pandemic period. Water electrolysis is one of the techniques capable of producing high purity, medical grade oxygen. The oxygen gas produced by electrolyser at low current densities typical of that encountered in a renewable energy coupled water electrolyser system consists of hydrogen impurity which can hinder continuous operation schedule of the system. A catalytic recombiner consisting of copper beads, catalytic and non-catalytic alumina beads is designed to mitigate hydrogen impurity present in the oxygen stream. Development of a CFD model is necessary to test certain Beyond Design Basis Accident (BDBA) scenarios which are not possible to be examined experimentally due to explosive nature of the gases. Accordingly, a CFD model is developed to predict the performance of packed bed reactor system under different modes of operation and at different impurity levels. The study recommends against the operation of reactor in the adiabatic mode or isothermal mode. In the adiabatic mode, very high temperatures are encountered at high hydrogen impurities whereas operation of the bed at coolant temperature, leads to water vapour condensation in the catalytic section thus impacting the hydrogen conversion rate. Hence, it is advisable to operate the reactor at temperatures above the expected dew point temperature of the gas mixture.

Keywords: Computational Fluid Dynamics Model, Catalytic Recombiner, Oxygen Purification, Packed Bed Reactor, Adiabatic Case, Isothermal Wall, Convective Heat Transfer

Introduction

During the present COVID – 19 pandemic, oxygen has become the most vital, life saving element of the periodic table. The conventional processes used for oxygen production are mainly based on separation of air using liquefaction or selective adsorption technique. The cryogenic air distillation process separates the constituents of air based on difference in their respective vapour pressures [1,2]. This technology has been the preferred choice for large- scale production of high purity oxygen to the tune of around more than 1000 MT/day[3]. On the other hand, the selective adsorption process makes use of synthetic zeolites like molecular sieves for preferential adsorption of air constituents based on their molecular diameter. This technology has the capability of producing oxygen at scale of 100 MT/day, however, the maximum purity attainable in a single cascade is limited to approximately 95%[3].

Water electrolysis is one of the non-conventional techniques for production of oxygen directly from water[4]. This non – air based process utilises DC electricity sourced from solar, wind, tidal or nuclear energy resources to split demineralised water into hydrogen and oxygen at near ambient conditions. The electrolyser can be operated in on demand and on site basis thus serving as both centralised as well as decentralised source for hydrogen and oxygen supply[5]. The hydrogen and oxygen gases produced by electrolysis method are relatively pure but require further purification as a polishing step for direct end use application. There is an inherent, small crossover of hydrogen and oxygen gases through the diaphragm employed in an electrolyser cell module. This could be attributed to the presence of slight differential pressure across the diaphragm. The mixing of gas soluble anolyte and catholyte is also cited as another reason resulting in increased hydrogen concentration in oxygen stream due to concentration gradient driven diffusion pathway[6].

Depending upon the construction, design and operation of the electrolyser cell, the hydrogen impurity in oxygen stream in industrial electrolysers is limited to 2%. The operation of electrolyser system at low current densities especially when coupled to renewable energy can lead to impurities beyond the set industrial range. This would severely affect and limit the operating schedule of the system thus interrupting vital oxygen flow from the electrolyser system[7].In order to avoid this scenario and ensure uninterrupted, prolonged operation of electrolyser without safety shutdown, the impure oxygen gas stream can be further purified using a passive method wherein the hydrogen impurity reacts with stoichiometric proportions of the bulk oxygen gas over a suitable catalyst in a reactor. This process is usually referred to as the catalytic recombination of hydrogen and oxygen gas to produce water using supported Platinum Group Metal (PGM) catalysts.

In the present study, the electrolyser operates at a low current density (2000 Ampere per square meter (ASM)) corresponding to 40% electrolyser loading. At this condition, the oxygen production flowrate is 2 Nm^3/hr and hydrogen impurity is considered to be up to 2.5%. A catalytic recombiner is designed in order to ensure continuous and complete conversion of hydrogen impurity. The model developed in this article analyses reactor behaviour in terms of temperature reached by the bed under different modes of operation and also at different impurity levels.

Estimation of packed bed flow parameters

The catalytic recombiner (CR) is a packed bed reactor which consists of sections of copper beads of 5 mm diameter, alumina beads and 0.5 % (w/w) Pd on alumina beads of approximately 4 mm diameter as catalyst for the recombination reaction.

The product gas from the electrolyser is moist and assumed to be fully saturated at 30 deg C. The corresponding water vapour is adsorbed in a silica gel – molecular sieve bed. The moisture-free gas then enters the CR filled with copper beads up to 100 mm length followed by 50 mm length each of catalytic and non-catalytic alumina beads. These are then followed by 100 mm length of copper beads as shown in the computational domain shown in Fig. 1.The non-catalytic alumina section downstream of the catalytic alumina section helps in slowing down the rate of heat transfer to coolant stream due to relatively lower thermal conductivity and higher heat capacity as compared to copper. As a result, moisture produced during recombination reaction is prevented from condensing over the catalytic section. This justifies the presence of a non-catalytic alumina section between the catalytic alumina and the copper beads section. An alternative arrangement is to introduce coolant stream near non-catalytic sections and provide heater with temperature controller over catalytic section in order to always maintain catalytic section at temperatures conducive to reaction kinetics.

The design of the reactor involves determination of diameter of the packed bed which meets the maximum pressure drop restrictions in the bed for a maximum feed gas flow rate corresponding to 2 Nm^3/hr.

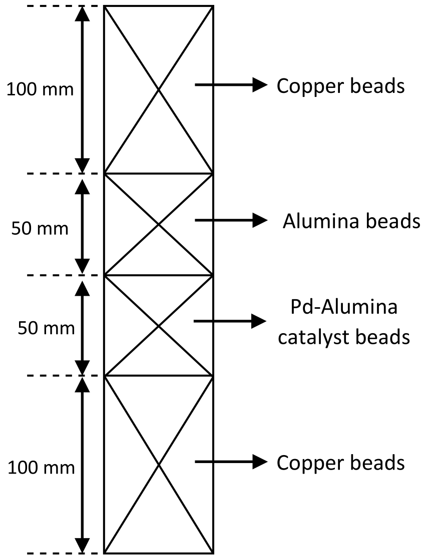

Fig.1: Geometry of problem domain

Pressure drop in a packed bed can be calculated using Ergun's equation (Equation (1)) which is a combination of Kozeny – Karman equation for laminar flow (1st term on R.H.S of Equation (1)) and Burke – Plummer equation (2nd term on R.H.S of Equation (1)) for turbulent flow of the reacting fluid *[8]*. The sphericity is taken as unity since spherical beads are assumed.

$$\frac{\Delta P}{L} = \frac{150\mu(1-\varepsilon)^2}{d_p^2\varepsilon^3}\bar{u} + \frac{1.75\rho(1-\varepsilon)}{d_p\varepsilon^3}\bar{u}^2 \qquad (1)$$

In this study, it is desirable to maintain laminar flow conditions in the bed to restrict the pressure drop values to a lower range. To ensure laminar flow conditions, the particle Reynolds number (Re_p) defined by Equation (2) should be less than 20*[9]*.

$$Re_p = \frac{d_p\bar{u}\rho}{\mu} = 20 \qquad (2)$$

At very low particle Reynolds number, the overall reaction may be controlled by external mass transfer effects. Since the concentration of impurities present in the oxygen gas stream is less, the thermo physical properties of pure oxygen gas are used for determination of dimensionless numbers, pressure drop, etc. Using Equation (2), the superficial velocity of oxygen gas stream is estimated which is later substituted in the Kozeny-Karman equation (Equation (3)) to evaluate the bed pressure drop. The bed porosity is estimated using the bulk and true density of alumina and copper beads Equation (4).

$$\frac{\Delta P}{L} = \frac{150\mu(1-\varepsilon)^2}{d_p^2\varepsilon^3}\bar{u} \qquad (3)$$

$$\varepsilon = 1 - \frac{\rho_B}{\rho_t} \qquad (4)$$

The bed diameter is calculated based on the superficial velocity of oxygen from Equation (5).

$$D = \sqrt{\frac{4Q}{\pi\bar{u}}} \qquad (5)$$

The reaction between hydrogen (H_2) and oxygen (O_2) is represented by Equation (6).

$$H_2 + \frac{1}{2}O_2 \longrightarrow H_2O, \Delta H_{ref} = -285\ kJ/mol \qquad (6)$$

Hydrogen acts as a limiting reactant in our case and due to low impurity levels, the reaction can be considered as a pseudo first order reaction with respect to hydrogen and can be expressed using Equation (7)*[10]*.The diffusion phenomenon is accounted by the apparent rate of recombination reaction consisting of both extrinsic as well as intrinsic mass transfer effects which are lumped together in the form of an effective activation energy and an effective pre-exponential factor as shown in Equation (7).

$$-r_{H2} = 1.96\ x\ 10^{11} exp\left(\frac{-73.77\ x\ 10^3}{RT}\right) C_{H2} \qquad (7)$$

The fractional change in the system volume is considered to be negligible considering the low concentration of hydrogen and water vapour as compared to oxygen.

Development of CFD model for catalytic recombiner

A CFD model is developed in order to evaluate the steady state performance of the reactor in beyond design basis events wherein the oxygen gas stream entering the reactor contains hydrogen impurity level of more than 4%.CFD becomes an important tool in studying such events since it is not safe and advisable to carry out experiments in explosive range of the gas mixture (4 – 96% H_2 in O_2).

The model is developed using a multi-physics approach to predict the performance of the recombiner system. The recombiner is modelled as a 2D axi-symmetric domain with the centre axial line of the reactor considered as r = 0. The recombiner model solves governing equations of flow, reactive species transport and energy balance in porous media. The governing equations of the model are described in subsequent sections.

The following assumptions have been made while developing the model:

1) Thermo physical properties of oxygen stream are considered to be constant with respect to the concentration of its constituents throughout the reactor. Hence, the density of the gas is assumed to be constant in the fluid flow equations. These properties are calculated for pure oxygen gas and are a function of temperature.

2) The effect of moisture in reduction of the catalytic activity is not considered in this model.

3) The back mixing effects are negligible in the packed bed.

4) The gas entering the reactor is assumed to be free from moisture. Hence, rate of reaction described by Equation (7) on dry basis can safely be used in the model.

5) All properties including bed porosity are considered to be isotropic.

Darcy's law (Momentum Conservation)

The Darcy's law describes fluid velocity through a packed bed in terms of viscosity of the fluid and permeability of the bed (Equation (8)). The equation indicates a linear relationship between the velocity and bed pressure drop*[11]*. This is obvious for laminar flow profile of a fluid passing through a packed bed. The Kozeny – Karman equation can be re-arranged and presented as Equation (9).

$$\bar{u} = -\frac{k}{\mu}\left(\frac{\Delta P}{L}\right) \tag{8}$$

$$\bar{u} = \frac{d_p^2\varepsilon^3}{150(1-\varepsilon)^2\mu}\left(\frac{\Delta P}{L}\right) \tag{9}$$

Comparing Equations (8) &(9), the bed permeability which is required as an input for the model can be determined (Equation (10)). This value is observed to be a function of the particle diameter and bed porosity.

$$k = \frac{d_p^2\varepsilon^3}{150(1-\varepsilon)^2} \tag{10}$$

A no slip boundary condition is applied at the wall as described by Equation (11) whereas a normal inflow velocity boundary condition (Equation (12)) is applied at the inlet of the reactor. The exit at top of the reactor is considered open to atmosphere ($p = 0$).

$$\bar{u} = 0 \tag{11}$$

$$-n.\bar{u} = u_0 \tag{12}$$

The velocity profile obtained from Darcy's law is used as an input for solving species and energy transport equations for estimation of the respective convective transfer phenomena whereas the temperature profile predicted by solution of energy transport equation helps in calculation of the temperature dependent thermo physical properties required for solving Darcy's law equation. The temperature profile also helps in determination of temperature dependent rate constant of the recombination reaction incorporated in the species transport equation. In this way, the developed model strongly couples the various physics involved in the recombination reactor.

Heat Transfer through Porous Media (Thermal Energy Conservation)

The heat transfer equation solved in the model is presented in Equation (13). Thermal conductivity and specific heat capacity of the bed is contributed by solid beads as well as oxygen gas stream flowing through it. Hence, effective thermal conductivity of the bed is described as a function of bed porosity and respective thermal conductivities of the beads and oxygen gas. Similarly, specific heat capacity of the bed $(\rho C_p)_{eq}$ is a function of bed porosity, respective heat capacities and densities of beads and oxygen gas as represented in Equation (14) [11].

$$\left(\rho C_p\right)_{eq}\bar{u}.\nabla T = \nabla.\left(k_{eq}\nabla T\right) + Q_s \tag{13}$$

$$k_{eq} = \varepsilon k_f + (1-\varepsilon)k_p \& \left(\rho C_p\right)_{eq} = \varepsilon\rho C_p + (1-\varepsilon)\rho_s C_{ps} \tag{14}$$

The heat of recombination reaction acts as a heat source for the packed bed reactor. Rate of heat transferred to the bed depends upon the reaction kinetics between hydrogen and oxygen and is expressed by Equation (15).The heat of reaction is calculated at steady state temperature attained by the system.

$$\overline{Q_s} = (-r_{H2}).\Delta H \tag{15}$$

The bed inlet boundary condition is fixed as T = 303 K. An outflow boundary condition as described by Equation (16) is applied to the bed outlet wherein heat transfer is only by convection.

$$-n.\left(-k_{eq}\nabla T\right) = 0 \tag{16}$$

The heat generated by the reactor is removed using chilled water which flows through a jacket enveloping the reactor bed. Three different heat transfer boundary conditions can be envisaged at the reactor wall during reactor operation:

(1) Constant heat transfer coefficient case: In this case, there exists a finite overall heat transfer coefficient which helps in transfer of heat from the reactor to the external cooling fluid. The boundary condition for this case is described by Equation (17). The heat transfer coefficient for present case is taken from literature *[12]*. In the present study, T_{ext} is considered to be 283 K.

$$-n.\left(-k_{eq}\nabla T\right) = h(T_{ext} - T) \tag{17}$$

(2)Adiabatic case: The reactor wall is considered to be thermally insulated to estimate maximum wall temperature for safety purposes. This situation arises when the cooling circuit has failed and developed a huge leak. In this case, the heat transfer from wall to surrounding chilled water does not take place. However, heat of recombination reaction continues to heat the beads and some amount of this heat is also carried away by the gas due to forced convection. The equation used to represent this condition at the wall is expressed as Equation (16).

(3) Constant wall temperature case: In this case, the reactor wall is maintained at a lower uniform temperature equivalent to the chiller water temperature. This case arises when the overall heat transfer coefficient is very high so that the cooling fluid is able to maintain a constant temperature ($T = T_{ext} = 283$ K) over the reactor wall.

Mass Transport through Porous Media (Mass Conservation)

Mass transfer phenomenon occurring within the packed bed reactor involves mass transfer due to diffusion, adsorption and convection along with back mixing effects, which is characterized by dispersion coefficient *[12]*. The participating species that are either produced or consumed during reaction are accordingly accounted by source or sink terms. The dispersion due to back mixing effects and mass transfer due to adsorption are assumed to be negligible to simplify the model. The internal diffusion phenomenon and external mass transfer effect are accounted by apparent rate of recombination reaction expressed by Equation (7)*[10]*. The intrinsic and extrinsic effects have been accounted in Equation (7). The mass conservation equations solved for i^{th} component are given by Equations (18) and (19).

$$\nabla.\bar{N_i} = S_i \tag{18}$$

$$\nabla.\bar{N_i} = \bar{u}.\nabla C_i \tag{19}$$

Source and sink terms are derived from the rate of reaction for the individual components as presented in Equation (20) *[13]*.

$$-(r_{H2}) = -2(r_{O2}) = (r_{H2O}) \tag{20}$$

A no-flux boundary condition for the species is applied at the reactor wall (Equation (21)). Inward flux of the individual species is specified at the bed inlet (Equation (22)) and outflow boundary condition describes the bed outlet (Equation (23)).

$$-n.\bar{N_i} = 0 \tag{21}$$

$$-n.\bar{N_i} = N_{0,i} \tag{22}$$

$$-n.D_i\nabla C_i = 0 \tag{23}$$

Results and Discussion

Pressure profile in the bed is presented in Fig. 2 (a) and Fig. 2 (b). The pressure drop in each section of the bed is different due to difference in bead diameter and bulk density of alumina (catalytic and non-catalytic) and copper beads. The main differentiating factor in Darcy's equation used in the model is permeability of the bed. Slope of the graph indicates resistance to fluid flow in the packed bed. The pressure drop is comparatively more in alumina bead (catalytic and non-catalytic) section due to low bed permeability value in that region.

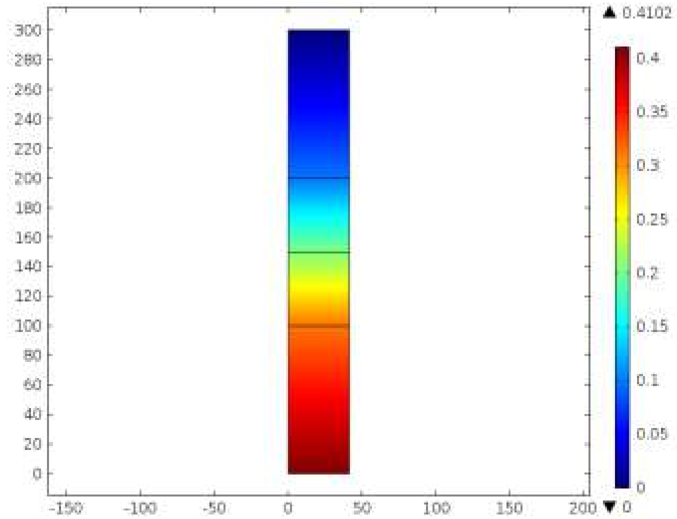

Fig.2 (a): Surface plot of pressure profile in the reactor (Pressure unit: Pa)

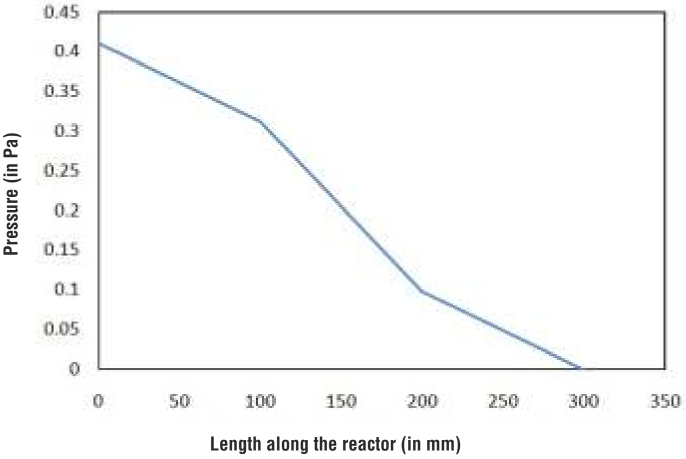

Fig.2 (b): Variation of pressure along the length of the reactor

Constant heat transfer coefficient case

The catalytic bed is cooled using chilled water to remove the exothermic heat of reaction. This will prevent overheating of catalyst and also avoid formation of hotspots in the bed. The overall heat transfer coefficient is considered to be approximately 285 W/m^2.Kwith chilled water inlet temperature of 283 K*[12]*. Accordingly, a convective heat flux boundary condition is employed at wall boundary to simulate dissipation of heat from bed to the coolant stream.

A grid independence test is essential to ensure that the simulation results are independent of the grid size. The mesh consists of unstructured triangular type mesh which is defined by the maximum and minimum element size. Analysis is carried out on the axial temperature plot of packed bed with maximum mesh element size ranging from 0.277 mm to 9.11 mm. The details of the various mesh element sizes used in this analysis are tabulated in Table 1. The maximum temperature predicted by the model is observed to be constant within acceptable limits for mesh sizes below 1.86 mm. This mesh size is used for further studies. The error is calculated by subtracting the corresponding temperature value from the successive value for the lower mesh and dividing the difference by value at the lower mesh.

Temperature profile in the bed for this condition with 2.5% hydrogen impurity in oxygen stream is shown in Fig. 3 (a) and Fig. 3 (b). A sharp increase in temperature is noticed when gas enters the catalyst section implying a rapid decrease in the hydrogen impurity content of the gas which is attributed to the high reaction

Table 1: Details of mesh element sizes

Sr. No.	Element size		No. of Domain elements	No. of boundary elements	Maximum Temperature (K)	Location of maximum (mm)	Error (%)
	Maximum (mm)	Minimum (mm)					
1.	9.11	0.29	448	93	316.1176	108.3155	0.79
2.	2.77	0.124	4184	291	318.6624	102.7698	0.09
3.	1.86	0.0828	9288	439	318.9506	101.8274	-0.085
4.	1.45	0.0414	15148	561	318.6812	101.4281	0.033
5.	0.277	8.28×10^{-4}	453686	2918	318.7862	101.9336	-

rate between oxygen and hydrogen. This effect is supported by the hydrogen conversion plotted in Fig. 4 for the catalytic alumina section. Heat generated by the catalyst is transferred by conduction to the upstream copper beads due to high conductivity of copper beads leading to preheating of the feed gas before it reaches the catalytic alumina bed. The high convective heat transfer coefficient ensures that the bed temperature decreases below the inlet gas temperature of 303 K near the catalytic alumina section.

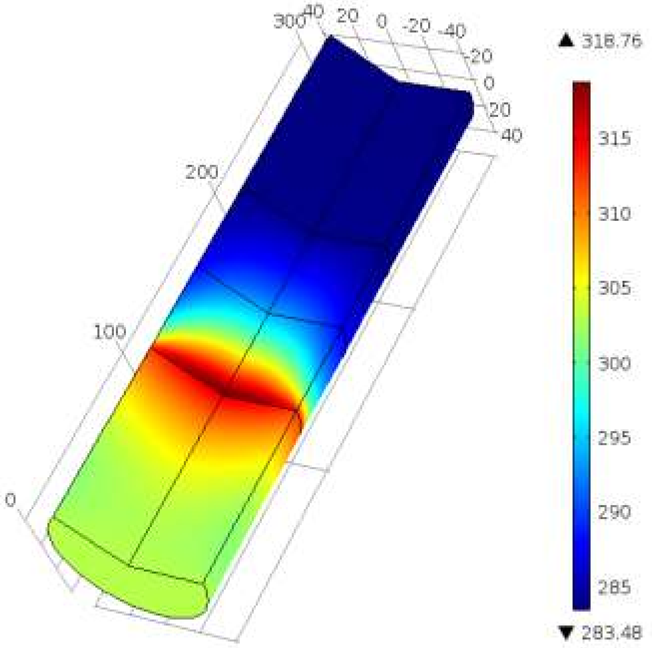

Fig. 3(a): Temperature profile in the reactor for constant heat transfer coefficient case (Temperature unit: K)

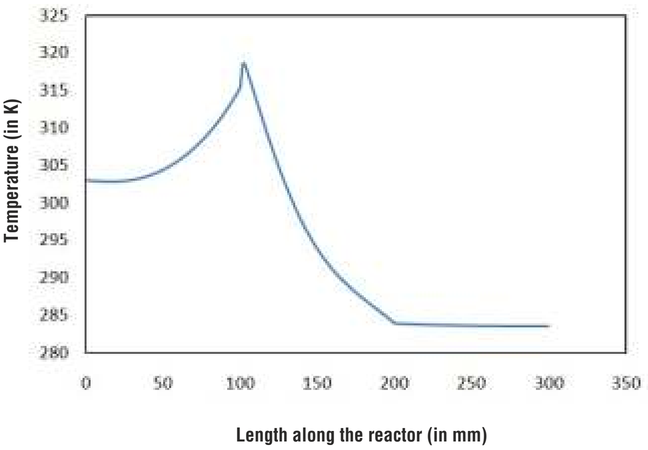

Fig. 3(b): Temperature along central axis of the reactor for constant heat transfer coefficient case

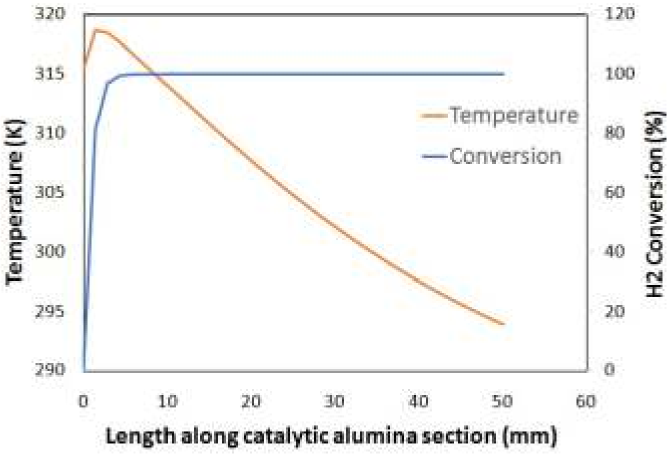

Fig. 4: Hydrogen conversion and temperature along central axis of the catalytic alumina section

The moisture content corresponding to 2.5% hydrogen impurity is equivalent to 2.5% in case of total conversion. This corresponds to a dew point of approximately 293 K. As seen in Fig. 3 (b), the temperature in the catalytic alumina section is observed to be above the corresponding dew point value, thus preventing condensation of water vapour on the catalyst. It is crucial to maintain the catalyst in a relatively dry state to avoid significant decrease in reaction rate which could further hamper the hydrogen conversion rate.

Adiabatic case

Chilled water supplied to the reactor is assumed to have failed in this case. The heat produced by the exothermic reaction is no longer dissipated to the coolant stream. To estimate the maximum temperature reached by the reactor wall, adiabatic boundary condition is considered at the wall. This expectedly leads to an increase in the central axial reactor temperature as compared to the convective heat transfer case as shown in Fig. 5 (a) and Fig. 5 (b).

The temperature rises steadily in the initial copper bead section, followed by a sharp increase at the beginning of the catalytic section which is later followed by a constant temperature regime in both the non-catalytic and copper bead section due to steady heat transfer by convection to the outgoing oxygen gas and by conduction to the non-catalytic alumina and copper bead section.

Since the present case results in higher bed temperatures, the model is used with hydrogen impurity varying from 1% to 10% to study the worst-case scenario expected in the bed. The results are presented in Fig. 6. It is observed that the maximum temperature encountered in the bed increases with increase in hydrogen impurity level in the feed, as is evident from Table 2.

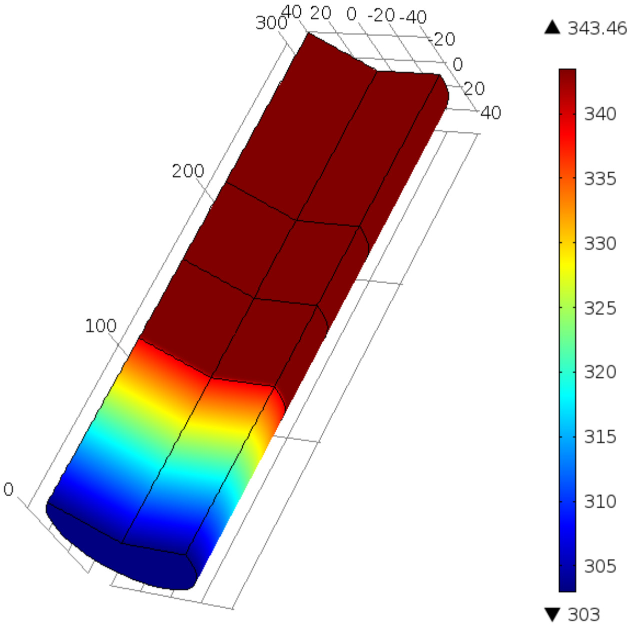

Fig. 5(a): Temperature profile of the reactor for adiabatic case (Temperature unit: K)

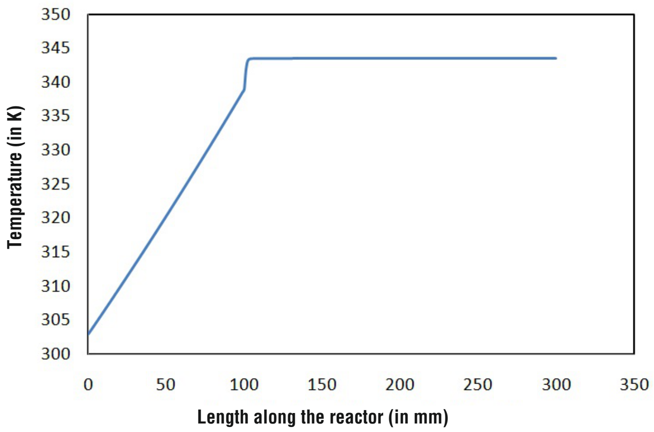

Fig. 5(b): Temperature alongcentral axis of the reactor for adiabatic case

Table 2: Overall rise in temperature at different hydrogen impurity levels for adiabatic reactor

H_2 impurity in O_2 stream (%)	**Overall rise in temperature ($T_{max} - T_{in}$) (^{0}C)**
1	17
2.5	40.46
5	75.67
7.5	107.44
10	136.71

Constant wall temperature case

In this case, it is assumed that the coolant flow rate is so high that temperature throughout the reactor wall is maintained at a constant value equivalent to the coolant inlet temperature. The temperature profile in the reactor and the temperature distribution along the reactor centre are plotted in Fig. 7 (a) and (b),respectively. It is observed that the copper beads in the initial section of the reactor rapidly cool the incoming oxygen gas, as a result of which the temperature of oxygen gas entering the catalytic alumina section is very low. A small spike in the gas temperature is observed in the catalyst section due to the exothermic reaction. Thereafter, the product gas temperature decreases gradually in the non-catalytic section followed by a quick decline in the last copper bead section.

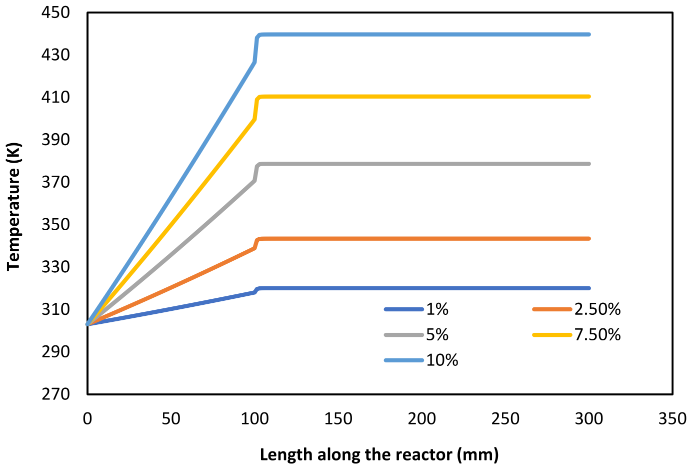

Fig. 6: Temperature along central axis of the reactor for adiabatic case with different hydrogen impurity levels

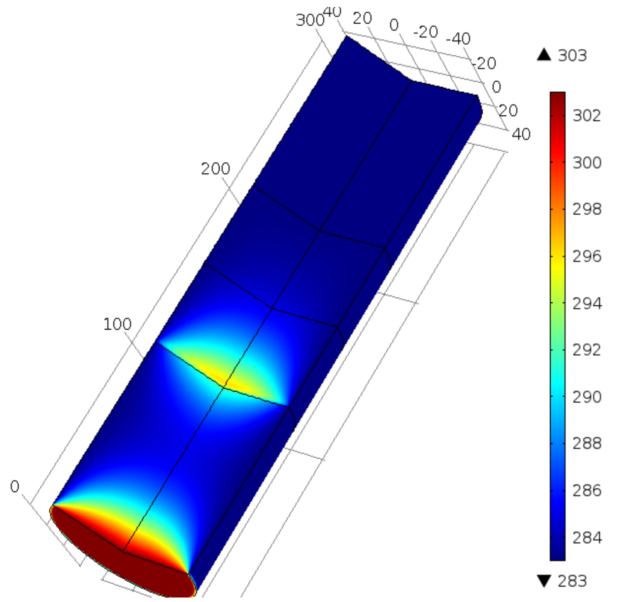

Fig. 7 (a): Temperature profile of the reactor for isothermal wall case (Temperature unit: K)

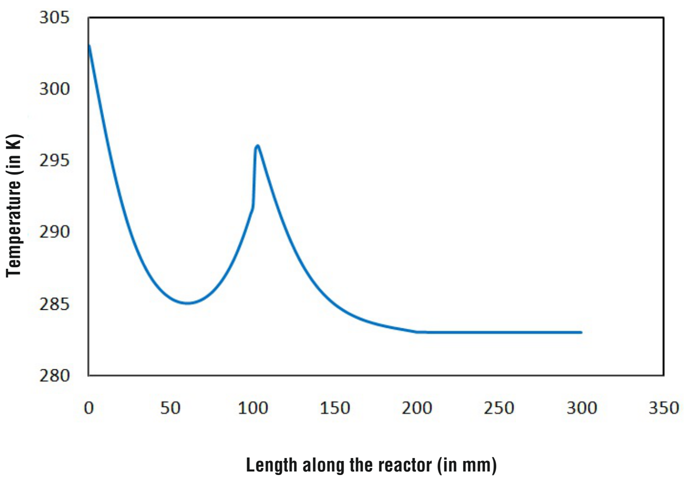

Fig. 7 (b): Temperature along central axis of the reactor in constant wall temperature case

It is important to note that temperature in bulk of the catalytic section is less than the dewpoint temperature of the product gas. This may lead to condensation of water vapours on the catalyst beads which would reduce the recombination reaction rate as well as hydrogen conversion. It is always desirable to maintain the bed temperature above dew point temperature of the product gas to avoid vapour condensation. Hence, it is recommended that the reactor should not be operated in this regime so that an appreciable rate of reaction and a significant conversion of hydrogen is achieved.

The reactor temperature profiles for all the above 3 cases are compared in Fig. 8. It is evident that the bed temperature in the isothermal wall case is lesser than that encountered for constant heat transfer coefficient case due to the presence of higher driving force for heat transfer in the isothermal wall case. As expected, higher bed temperature is reached by the bed when adiabatic boundary condition is imposed on the reactor wall.

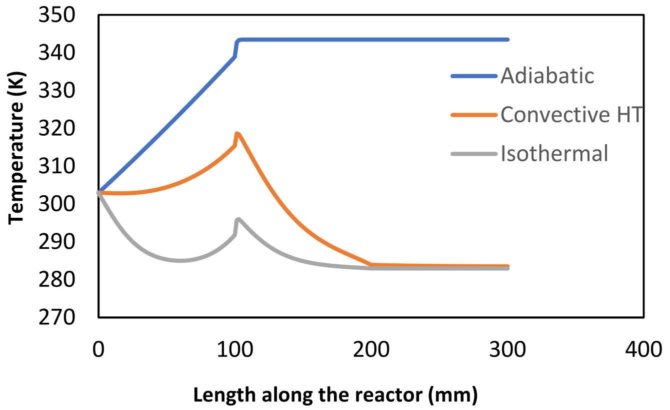

Fig. 8: Temperature along central axis of the reactor for all 3 cases compared in this study

Conclusion

A model for predicting the performance of a packed bed catalytic recombiner in terms of pressure drop, temperature and hydrogen conversion has been developed. Performance of the reactor under the three modes of operation has been evaluated. The behaviour of reactor at different hydrogen impurities in the adiabatic case is also considered in the present study. In adiabatic case, very high temperatures are experienced in the bed whereas in isothermal wall case, the catalyst section encounters temperatures lower than the dew point which could lead to water vapour condensation on catalyst thereby reducing the recombination rate. Hence, the reactor operation in either of these modes should be avoided. This study recommends operation of reactor at temperatures above dew point temperature especially in the catalytic section in order to achieve complete conversion of hydrogen.

As a part of future studies, an experimental system of the recombination reactor would be set up and tested under safe, normal operating conditions. The data from the experimental test set up would be used for validation of the simulation results.

Acknowledgement

The authors acknowledge the requisite computing support provided by Dr. K.K. Singh, Chemical Engineering Division (ChED), BARC.

Notations

ε	Bed porosity	-
μ	Fluid viscosity	Pa.s
ρ	Density of oxygen stream	kg/m^3
ρ_s	Density of beads	kg/m^3
ρ_B	Bulk density of copper/ alumina beads	kg/m^3
ρ_t	True density of copper/ alumina beads	kg/m^3
C_i	Concentration of i^{th} species	mol/m^3
C_{H2}	Concentration of hydrogen	mol/m^3
C_p	Specific heat capacity of oxygen stream	kJ/kg.K
C_{ps}	Specific heat capacity of beads	kJ/kg.K
d_p	Diameter of copper/ alumina bead	m
D	Diameter of packed bed	m
D_i	Diffusivity of i^{th} species	m^2/s
H	Heat transfer coefficient	W/m^2.K
ΔH	Heat of reaction	kJ/kmol
k	Bed permeability	m^2
k_{eq}	Equivalent thermal conductivity of packed bed	W/m.K
k_f	Thermal conductivity of fluid	W/m.K
k_p	Thermal conductivity of copper/ alumina bead	W/m.K
L	Length of packed bed	m
$\bar{N_i}$	Total flux of i^{th} species	mol/m^2.s
$N_{0,i}$	Flux of i^{th} species at bed inlet	mol/m^2.s
P	Pressure	Pa
Q	Volumetric flowrate of gas	m^3/s
Q_s	Volumetric heat generation rate	W/m^3
$-r_{H2}$	Apparent rate of consumption of hydrogen	mol/m^3.s
r_{H2O}	Apparent rate of production of water vapour	mol/m^3.s
$-r_{O2}$	Apparent rate of consumption of oxygen	mol/m^3.s
R	Universal gas constant	kJ/kmol.K
Re_p	Particle Reynolds number	-
S_i	Rate of production/ consumption of i^{th} species	mol/m^3.s
T	Temperature	K
T_{ext}	External temperature	K
$\bar{u}$	Superficial gas velocity	m/s
u_0	Superficial gas velocity at inlet	m/s

Corresponding Author*

Sachin Kamath (sachin@barc.gov.in)

References

[1] Industrial Oxygen: Its Generation and Use, ACEEE Summer Study on Energy Efficiency in Industry, 2007.

[2] Improved Oxygen Production Technologies, IEA Green House Gas R&D Programme, 2007, 14.

[3] Emerging and Existing Oxygen Production Technology Scan and Evaluation, COSIA, GHG Working Group, 2018.

[4] Takeyoshi Kato, Mitsuhiro Kubota, Noriyuki Kobayashi, Yasuo Suzuoki, *Energy.*,2005, **30**, 2580.

[5] K.C. Sandeep, Sachin Kamath, Krunal Mistry, Ashok Kumar M, S.K. Bhattacharya, Kalyan Bhanja, Sadhana Mohan, *Int. Journal of Hydrogen Energy*, 2017 **42**, 12094.

[6] Jörn Brauns, Thomas Turek, *Processes.*, 2020, **8**, 248.

[7] Philipp Haug, Matthias Koj, Thomas Turek, *Int. Journal of Hydrogen Energy.*, 2017, **42**,9406.

[8] Warren L. McCabe, Julian C. Smith, Peter Harriott, Unit Operations of Chemical Engineering, McGraw-Hill International, Fifth edition., 1993.

[9] O. Levenspiel, Engineering Flow and Heat Exchange, Springer, Third edition., 2014.

[10] K.C. Sandeep, Rupsha Bhattacharyya, Chandrashekhar Warghat, Kalyan Bhanja, Sadhana Mohan, *Int. Journal of Hydrogen Energy*, 2014, **39**, 17906.

[11] COMSOL Multiphysics documentation.

[12] Convective Heat Transfer Coefficients Table Chart, www.engineersedge.com/heat_transfer/convective_heat_transfer_coefficients__13378.htm

[13] O. Levenspiel, Chemical Reaction Engineering, Wiley, Third edition, 1998.